JACS
JOURNAL OF THE AMERICAN CHEMICAL SOCIETY
Article
pubs.acs.org/JACS

Photocatalytic Metal–Organic Framework from CdS Quantum Dot Incubated Luminescent Metallohydrogel

Subhadeep Saha, Gobinda Das, Jayshri Thote, and Rahul Banerjee*

Physical/Materials Chemistry Division, CSIR-National Chemical Laboratory, Dr. Homi Bhabha Road, Pune 411008, India

Supporting Information

ABSTRACT: Cadmium sulfide (CdS) quantum dots (<10 nm in size) have been successfully synthesized in situ without any capping agent in a Zn(II)-based low-molecular-weight metallohydrogel (ZAVA). Pristine ZAVA hydrogel shows blue luminescence, but the emission can be tuned upon encapsulation of the CdS quantum dots. Time-dependent tunable emission (white to yellow to orange) of the CdS incubated gel (CdS@ZAVA gel) can be attributed to sluggish growth of the quantum dots inside the gel matrix. Once CdS quantum dots are entrapped, their augmentation can be stopped by converting the gel into xerogel, wherein the quantum dots remains embedded in the solid xerogel matrix. Similar size stabilization of CdS quantum dots can be achieved by means of a unique room-temperature conversion of the CdS incubated ZAVA gel to CdS incubated MOF (CdS@ZAVCl) crystals. This in turn arrests the tunability in emission owing to the restriction in the growth of CdS quantum dots inside xerogel and MOF. These CdS embedded MOFs have been utilized as a catalyst for water splitting under visible light.

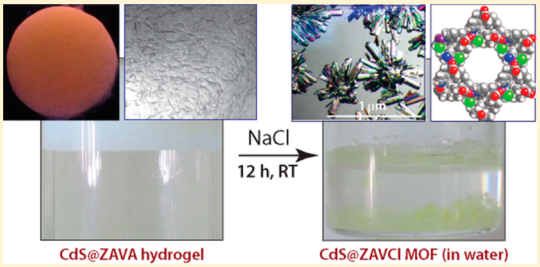

INTRODUCTION

Gels are composed of solid gelators and liquid constituents immobilized by surface tension.[1] The gelators (predominantly polymeric species) form continuous, three-dimensional cross-linked fibrillar structures which span through the matrix, allowing a large amount of liquid to get ensnared inside the voids.[2] Apart from the conventional polymeric gelators, low-molecular-weight gelators (LMWGs) have attracted much attention in the past decade thanks to their potential applications in catalysis, biomedicines, and nanoelectronics.[3] Additionally, LMWGs have earned recognition as hosts for various inorganic nanomaterials such as noble-metal nanoparticles and metal chalcogenide quantum dots (CdS, CdTe).[4] The intention behind incorporation of the inorganic nanoparticles in the gels is to make an attempt to organize these nanoparticles on the 3D gelator matrix in order to tune the properties of the nanoparticles.[5] However, one finds limited examples of such composite materials with a promising property that could fulfill the need for construction of such functional materials.[6]

Herein, we report a simple one-pot synthesis as well as entrapment of uncapped CdS quantum dots in a low-molecular-weight metallohydrogel (ZAVA). This CdS incubated luminescent metallohydrogel (CdS@ZAVA gel) can easily be transformed into its dry xerogel form (CdS@ZAVA xerogel), which also shows luminescence. Moreover, this metallohydrogel (CdS@ZAVA) can be converted toa luminescent CdS embedded metal–organic framework (ZAVCl MOF) via a unique sodium chloride mediated room-temperature process. Metal–organic frameworks (MOFs) are crystalline porous materials which show promising applications in the fields of gas storage, separation, catalysis, drug delivery, and proton and charge carrier transport.[7] These crystalline materials are mainly synthesized by hydrothermal,[7a,c] room temperature,[7j,k] or mechanochemical[7l] methods. However, the gel-mediated crystal growth process, which has been regarded as one of the most efficient methods to synthesize a wide variety of important crystalline materials such as metal oxides, zeolites, and organic molecules,[8] has rarely been attempted to synthesize MOFs. In this present work we have made an attempt to provide a simple, first of its kind, single-step recipe to obtain high-quality MOF single crystals at room temperature via destruction of a low-molecular-weight metallohydrogel, ZAVA. It is to be noted that Yaghi et al. were the first to synthesize a MOF utilizing a gel-mediated crystal growth procedure by using nonaqueous poly(ethylene oxide) (PEO) gel as an inert matrix.[9] In addition to that, Steed and co-workers used low-molecular-weight organogels as inert gel matrixes to synthesize single crystals of a range of important organic molecules, including APIs.[10]As mentioned before, we could load uncapped CdS quantum dots in the metallohydrogel matrix and subsequently utilize this CdS@ZAVA metallohydrogel to synthesize MOF-CdS quantum dot composite single crystals. The other MOF–quantum dot composites found in the literature[11] have been prepared via a multistep, energy-expensive procedure. To the best of our knowledge, this kind of in situ loading of quantum dots in the MOF via degradation of a quantum dot loaded gel is unprecedented. This composite MOF (CdS@ZAVCl) can be used as an efficient catalyst for a

Received: July 15, 2014
Published: October 3, 2014

   dx.doi.org/10.1021/ja509019k | J. Am. Chem. Soc. 2014, 136, 14845–14851

visible light driven water splitting reaction for the production of hydrogen gas.[12]

EXPERIMENTAL SECTION

The preparation of amino acid based ligands,[13] the synthesis of ZAVA gel, xerogel,[14] CdS@ZAVA gel, xerogels, ZAVCl, and CdS@ZAVCl MOFs, photocatalytic reactions, and Mott–Schottky experimenst have been detailed in the Supporting Information.

RESULTS AND DISCUSSION

In general, entrapment of quantum dots in a gel (or any host matrix; e.g. MOFs etc.) requires two steps: (i) synthesis of quantum dots in the presence of capping agent (to avoid agglomeration to bigger particles) and (ii) entrapment of these quantum dots in the host matrix during its synthesis.[11] In contrast, the synthesis of CdS@ZAVA gel provides a unique way for the one-pot synthesis of functional composite materials containing CdS quantum dots. This composite material shows tunable luminescence properties (white to yellow to orange) as a consequence of a slow agglomeration process of the entrapped quantum dots with time (Figure 1). However, the

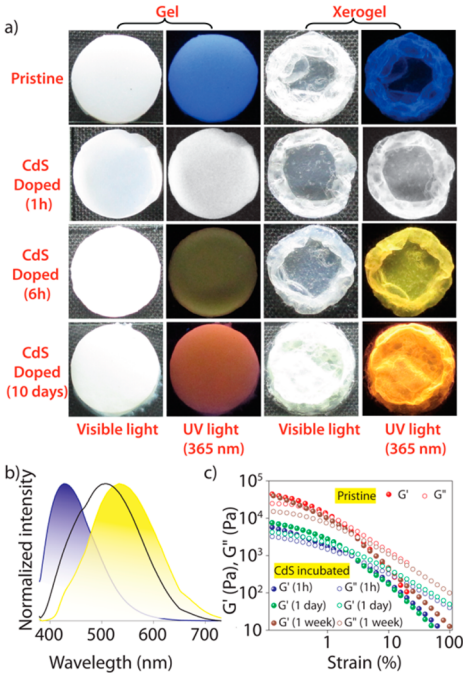

Figure 1. (a) Pristine and CdS incubated ZAVA gel and xerogels under visible light and UV light (365 nm). (b) PL spectra of pristine and CdS loaded ZAVA xerogels. Blue indicates the pristine xerogel, and black indicates the white emitting and yellow the yellow luminescent CdS doped xerogel at 365 nm excitation. (c) Strain sweep test for pristine ZAVA gel and CdS incubated ZAVA gel at different times after doping of CdS.

growth of the quantum dots and the luminescence color of the composite gel can be restricted by converting this gel to solid xerogel. ZAVA xerogel shows a transformation to the original gel phase upon addition of an equal amount of water extracted while vacuum drying. This suggests that a vacuum drying process does not destroy the integrity of the material. Scheme 1 illustrates the rapid formation of ZAVA hydrogel upon mixing of two stock aqueous solutions containing ZA and VA, via the formation of a transient colloidal suspension phase. In addition to that, a CdS@ZAVA gel can be obtained if aqueous solutions

Scheme 1. Schematic Representation of Synthesis of the Pristine ZAVA Gel and CdS Incubated ZAVA Gel

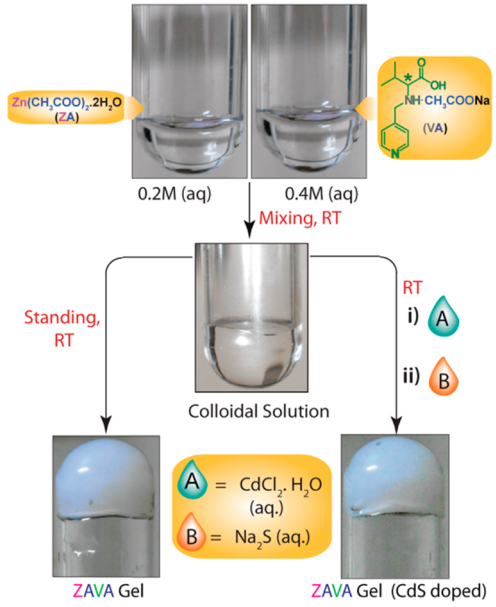

of $CdCl_2 \cdot H_2O$ and $Na_2S \cdot xH_2O$ were added to the aforementioned ZAVA colloidal suspension one after another with vigorous shaking. Unlikethe typical heating–cooling protocol, the gelation phenomenon illustrated here takes place efficiently at room temperature (25–30 °C). This combination of metal salt (ZA) and ligand (VA) does not form a gel in most protic and aprotic solvents (please see Table S1 in the Supporting Information for solvents that have been tried for gelation) but water. This feature can be explained by means of the H bond donor[15] (N_{amine}–H···O_{water}) and acceptor (O_{water}–H···$N_{pyridine}$) nature of the gelator complex (Figure S1, Supporting Information). The organic part (VA) of the gelator contains an amine functionality in protonated form ($-NH_3^+$), which can act as an H bond donor by accepting a lone pair of electrons from an electronegative element (e.g., oxygen of water) via its electron-deficient proton to form H bonds. It (VA) also contains a pyridine functionality which can act as an H bond acceptor. Hence, for gelation to take place efficiently, a solvent such as water is needed which is capable of acting as both an H bond donor (α = 1.17) as well as acceptor (β = 0.47).[16] This results in the assembly of water molecules and gelator complexes, leading to the formation of a gel network. The ligand VA forms precipitates with most of the other metal salts (e.g., common salts of Ca(II), Mg(II), Al(III), Fe(III/II), Co(II/III), Ni(II), etc.) but forms gels in water with zinc nitrate hexahydrate ($Zn(NO_3)_2 \cdot 6H_2O$ = ZN as ZNVA gel) and zinc perchlorate hexahydrate ($Zn(ClO_4)_2 \cdot 6H_2O$ = ZP as ZPVA gel). $Zn(NO_3)_2 \cdot 6H_2O$ and $Zn(ClO_4)_2 \cdot 6H_2O$ failed to form any gel with VA ligand in the presence of Na_2S.[17]

As mentioned in the Experimental Section, in order to obtain CdS incubated ZAVA gel, first the aqueous solution of $CdCl_2$ and then the aqueous solution of Na_2S have to be added to the colloidal solution one after another. In this process, the gelator complex is allowed to form first. $CdCl_2$ is not recommended to be added in the beginning while ZA and VA solutions are mixed to avoid an unwanted reaction between Cd^{2+} and VA. After addition of $CdCl_2$ to the colloidal solution, Na_2S has to be added dropwise with vigorous shaking, as a sudden addition would cause an unwanted formation of ZnS as a precipitate. On

dx.doi.org/10.1021/ja509019k | J. Am. Chem. Soc. 2014, 136, 14845–14851

the other hand, large particles of ZnS (>50 nm) form (see Figure S2 in the Supporting Information) if the addition of $CdCl_2$ is skipped and only Na_2S is added directly to the colloidal solution immediately after mixing of ZA and VA solutions. Further studies (vide infra) established that the incorporated CdS particles are <10 nm sized CdS quantum dots. To the best of our knowledge, this is a rare one-pot synthesis and entrapment procedure of any semiconductor quantum dot in a gel matrix without any capping agent. There is only one report in the literature which describes a complex multistep synthesis of a CdTe nanocrystal doped Cd^{2+} based hydrogel.[18] The ability of ZAVA gel to immobilize CdS particles of <10 nm size can be attributed to the presence of a pyridine moiety in the VA ligand. Recent reports[19] on nucleotide (e.g., ATP, adenosine triphosphate) passivated nanocrystals have shown that the pyridinic nitrogens of adenine bind to the metal ions of inorganic nanocrystals to restrict their growth to larger clusters. We assume that the pyridinic nitrogen of the VA ligand, which takes part in H bonding in the ZAVA gel network, binds to the Cd^{2+} ion of the CdS quantum dots and stabilizes the quantum dots within the gel matrix.

All of the materials discussed above (pristine and CdS incubated gel, xerogel) appear white under visible light, but they exhibit different luminescence colors under UV light (Figure 1a). The as-synthesized ZAVA gel and xerogel exhibit strong blue luminescence (Figure 1) under UV light (365 nm) with PL maxima (λ_{em}) of 437 and 429 nm, respectively (Figure S3 (Supporting Information) and Figure 1b). Surprisingly, the luminescence color and PL maxima of the ZAVA gel change abruptly upon doping of CdS in the ZAVA gel matrix. The luminescence color of the CdS@ZAVA gel changes from blue to white upon standing at room temperature for ∼1 h after doping of CdS. The PL spectrum also changes accordingly and exhibits a broad spectrum, consisting of two humps having maxima at 434 and 548 nm, covering the entire visible region (Figure S3). This particular state of CdS@ZAVA gel reveals CIE coordinates (0.30, 0.35) (Figure S3) which are ideal for white emission in accordance with the 1931 CIE coordinate diagram.[20] This transformation can be attributed to the transfer of energy between two chromophoric units (ZAVA gel acts as a donor and CdS quantum dots act as acceptor chromophores) present in the system (see section S4 in the Supporting Information). The corresponding xerogel obtained from white-emitting CdS@ZAVA gel also exhibits white luminescence (CIE coordinates (0.25, 0.31); Figure S3) under 365 nm UV light. The PL spectrum also shows a broad spectrum covering the whole visible region, as evidenced in the case of CdS@ZAVA gel (Figure 1b). The luminescence color of the CdS@ZAVA gel appears to be transient and gradually changes to yellow (after ∼6 h) followed by orange (after ∼10 days) presumably due to the slow aggregation process of the CdS quantum dots in the gel matrix. Yellow and orange luminescent gels were also found to yield xerogels of similar luminescent color (Figure 1a,b).

The viscoelastic gel nature of ZAVA and its CdS incubated analogues was confirmed from their mechanical properties in dynamic rheological experiments (Figure 1c). Both pristine ZAVA gel and CdS@ZAVA gel were characterized by an average storage modulus (G') higher than the loss modulus (G'') within the linear viscoelastic regime (pulsation ω = 10 rad s^{-1}; strain 0.1%), as determined by dynamic strain sweep measurements (range 0.1−100%; Figure 1c). However, CdS@ZAVA gel was found to be weaker in nature than pristine ZAVA gel (after 1 h of doping), as it exhibits a 1 order of magnitude lower storage modulus value (G') than the pristine gel. It is noteworthy that the mechanical properties of CdS@ZAVA change with time and become comparable to those of the pristine ZAVA gel after 1 week of aging (Figure 1c). This improvement proves that incubation of CdS cannot affect the mechanical strength of the gel, even though some pyridinic N becomes involved in capping the CdS quantum dots instead of participating in H bonding, as the loading of CdS is very low (∼1.26 wt %). The FTIR patterns of ZAVA xerogel do not differ from those of its CdS incubated counterpart (Figure S6, Supporting Information), which proves that the chemical identity of the xerogel remains intact even after doping of CdS. The PXRD patterns of the xerogel samples (pristine and CdS incubated) reveal their amorphous nature. The presence of crystalline CdS quantum dots does not influence the PXRD patterns of the xerogel samples (Figure S6) owing to the very small amount of loading (∼1.26 wt %) of CdS quantum dots in the gel matrix. In terms of stability, ZAVA remains visually intact upon standing at room temperature in an airtight container for more than 1 year without any significant change in appearance. It gradually solubilizes in water within ∼24 h (2 mL of gel in 4 mL of water). With regard to the thermal stability, thermogravimetric analysis (TGA, under an N_2 atmosphere; Figure S6) of the xerogel samples (both pristine and CdS incubated) initially exhibits a steady weight loss of ∼20% up to 270 °C, illustrating the loss of water followed by degradation of unreacted ligand (mp of VA 154 °C). The sudden weight loss starts at 270−280 °C (∼40%) until 470 °C gives the destruction of the gel network. As expected, the CdS@ZAVA xerogel yields a greater amount of leftover mass (∼8 wt %) than the pristine gel, as the former contains CdS along with ZnO, which comes from pyrolysis of the xerogel part (up to 800 °C). We took transmission electron microscopy (TEM) images to obtain insights into the microstructures as well as distribution of CdS quantum dots in CdS@ZAVA xerogel (Figure S2, Supporting Information). The interwoven nanofibrillar morphology of CdS@ZAVA xerogel was visible in the TEM image (Figure S2). High-resolution TEM images show the distribution of <10 nm sized CdS quantum dot particles embedded on the gel fibers. This CdS quantum dot particles exhibit a lattice spacing of 0.336 nm, indicative of the distance between two adjacent (111) planes of cubic CdS (JCPDS Card No. 75-1546; Figure S2).

CdS quantum dots are well-known low band gap semiconductor materials which have the ability to absorb light in the visible region. Hence, these quantum dots are used as a photosensitizer in several composite photocatalysts used in visible light water splitting reactions.[12] However, the direct use of either of these two composites (CdS@ZAVA gel and its xerogel) as a photocatalyst for the water splitting reaction is practically impossible, as the gel dissolves in water and the xerogel forms a gel in the presence of water. This problem provoked us to synthesize a water-stable CdS loaded material. We have recently reported that ZAVCl-MOF,[13c] which has been synthesized using zinc acetate dihydrate as the metal ion precursor and a ligand similar to VA (mixture of (V = L-3-methyl-2-(pyridin-4-ylmethylamino)butanoic acid and sodium chloride), is stable in water. The crystal structure of ZAVCl-MOF reveals the presence of a chloride ion in the coordination environment of Zn^{2+} along with two oxygens (from two carboxylates) and two nitrogens (one from pyridine and one from the amine of the ligand).[13c] We exploited this knowledge

dx.doi.org/10.1021/ja509019k | J. Am. Chem. Soc. 2014, 136, 14845−14851

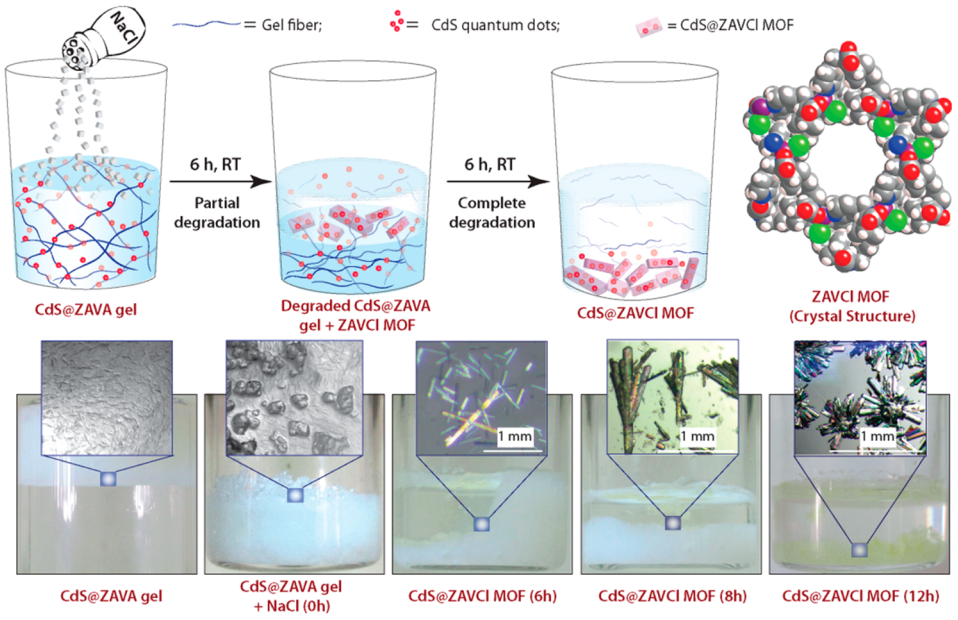

Figure 2. (top) Schematic representation of production of CdS loaded ZAVCl MOF (CdS@ZAVCl-MOF) from CdS loaded ZAVA gel (CdS@ZAVA gel) and space-filling representation of the crystal structure of ZAVCl (view through *c* axis. Color code: carbon, gray; hydrogen, white; zinc, purple; chlorine, green; nitrogen, blue; oxygen, red. (bottom) Real-time digital photographs of CdS@ZAVA gel to CdS@ZAVCl MOF conversion process.

to synthesize ZAVCl-MOF from ZAVA gel by the simple addition of chloride salt (NaCl, KCl, NH_4Cl, etc.) at room temperature. It is worth pointing out that this "room-temperature gel to crystal" method yields millimeter sized rod-shaped, transparent ZAVCl-MOF crystals (Figure 2), in contrast to the conventional solvothermal method, which gives much smaller crystals (~50 μm) under high-temperature conditions (90 °C).[13c] CdS@ZAVA gel faces a similar fate as ZAVA gel in the presence of NaCl, producing CdS quantum dot embedded ZAVCl-MOF crystals (Figure 2) at room temperature. To the best of our knowledge, this is the easiest immobilization procedure of any quantum dot nanoparticle in MOF matrix to date.[11] These CdS quantum dots do not reside inside the pore of the MOF (pore diameter 1.2 nm), as they are larger (5−9 nm) than the pore. They also do not adhere on the outer surface of the crystal, as their photoluminescence and their photocatalytic activity do not change even after several washings in water. Hence, these quantum dots are presumably sandwiched between crystallite surfaces of ZAVCl-MOF.[11c]

As expected, FTIR patterns of ZAVCl-MOF and CdS@ZAVCl-MOF do not differ much from each other (Figure S6, Supporting Information). The PXRD pattern (Figure 3a) of ZAVCl-MOF shows that it is highly crystalline in nature and this very nature remains unaltered upon loading of CdS, as the amount of loading (~1%) is much less. As experienced in the case of CdS@ZAVA xerogel, ZAVCl-MOF also exhibits weight loss in two stages, (i) ~3% (loss of water present in the framework; at 98−100 °C) and (ii) ~45% (260−270 °C, which can be attributed to the framework collapse), respectively. In this case also the CdS incubated material (CdS@ZAVCl MOF) produces more leftover mass (~11 wt %) in comparison to that for the pristine gel for a reason similar to that described in the case of CdS@ZAVA xerogel. Similar to the case for pristine ZAVA gel, pristine ZAVCl-MOF also shows blue luminescence under UV excitation (365 nm, Figure 3b,c,f). Similarly, white luminescent CdS@ZAVA gel can be transformed into white

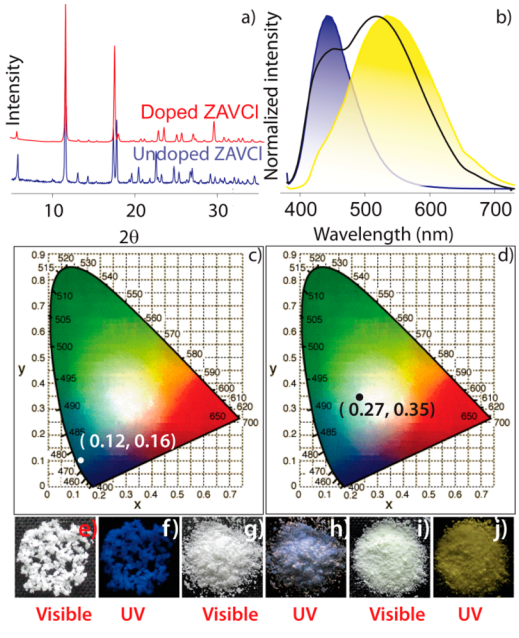

Figure 3. (a) PXRD spectra of ZAVCl-MOF and CdS@ZAVCl-MOF. (b) PL spectra of pristine ZAVCl-MOF (blue), white luminescent CdS@ZAVCl-MOF (black), and yellow luminescent CdS@ZAVCl-MOF (yellow) under 365 nm UV excitation. (c, d) CIE chromaticity diagrams of (c) pristine ZAVCl-MOF (blue luminescent) and (d) CdS@ZAVCl-MOF (white luminescent). (e−j) Digital photographs of pristine ZAVCl-MOF (e) under visible light and (f) under 365 nm UV light, white luminescent CdS@ZAVCl-MOF (g) under visible light and (h) under UV light (365 nm), and yellow luminescent CdS@ZAVCl-MOF (i) under visible light and (j) under UV light (365 nm).

luminescent MOF (CIE coordinates (0.27, 0.35); Figure 3d) upon reaction with NaCl. Moreover, the CdS@ZAVCl MOF derived from yellow CdS@ZAVA gel also shows yellow luminescence color under UV light. This transformation of

dx.doi.org/10.1021/ja509019k | J. Am. Chem. Soc. 2014, 136, 14845−14851

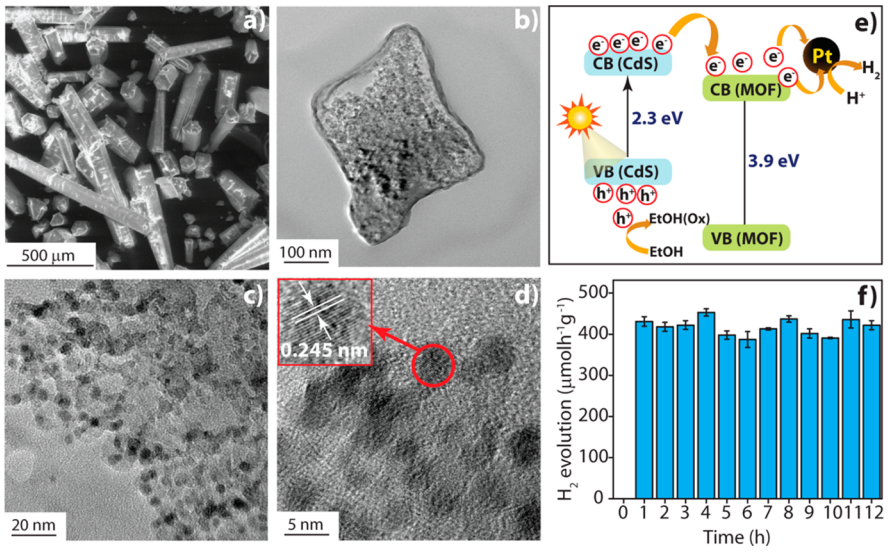

Figure 4. (a) SEM images of CdS@ZAVCl and (b–d) TEM images of CdS@ZAVCl-MOF. (e) Mechanism of water splitting by CdS@ZAVCl photocatalyst (30 mg), with 0.5 wt % cocatalyst Pt and λ >420 nm. (f) Stability test of the photocatalyst (CdS@ZAVCl-MOF) in 12 cycles of the water splitting reaction.

the photoluminescence color of ZAVCl MOF upon doping of CdS quantum dots can be attributed to the possible energy transfer between the donor (ZAVCl MOF) and acceptor chromophore (CdS quantum dots) present in the composite (CdS@ZAVCl MOF; see section S4 in the Supporting Information for further details). The PL spectra as well as the CIE chromaticity diagrams of all the materials (pristine and CdS incubated gel, xerogel, and MOF materials) have been detailed in Figure S3 in the Supporting Information. SEM images of the MOF crystals show rodlike morphology of the ZAVCl-MOF crystals (Figure 4a). To probe the distribution and nature of CdS quantum dots in the MOF matrix, we took HRTEM images of CdS@ZAVCl MOFs. They also reveal a decent distribution of <10 nm sized particles (7–9 nm) engraved in the crystal matrix (Figure 4b–d) having a lattice separation of 0.245 nm (*d* spacing between two (102) planes of hexagonal CdS crystals; JCPDS Card No. 41-1049). TEM-EDAX (Figure S8, Supporting Information) exhibits ∼1% loading of CdS in CdS@ZAVCl-MOF (although ICP-AES analysis shows a loading of 0.52–0.72 wt %.)

Finally, the well-known photosensitizing ability of low band gap, visible light active CdS quantum dots motivated us to check the photocatalytic activity of such CdS-loaded ZAVCl-MOF. The photocatalytic H_2-production ability of the prepared CdS@ZAVCl MOF was determined under visible light irradiation using Pt as a cocatalyst and ethanol as a sacrificial reagent. The sacrificial reagent (ethanol) consumes photogenerated holes to prevent the photocatalyst from photocorrosion.[12a] Control experiments (in the absence of either irradiation or photocatalyst) indicated no significant production of hydrogen, which indicates that H_2 was produced via a photocatalysis reaction on the photocatalyst. It was observed that the binary composite (CdS@ZAVCl), with size distribution ranging between 7 and 9 nm, showed H_2 production on illumination of visible light (398–418 μmol h^{-1} g^{-1} or 39.8–41.8 mmol h^{-1} $g_{CdS}{}^{-1}$, considering that the doping of CdS inside MOF is ∼1 wt %). To determine the influence of the MOF on the encased CdS quantum dots, thioglycolic acid capped CdS nanoparticles (7–8 nm particle size) were separately synthesized. Notably enough, both pristine ZAVCl (18 μmol h^{-1} g^{-1}) and thioglycolic acid capped CdS quantum dots (100 μmol h^{-1} g^{-1}) showed lower H_2 evolution efficiency than CdS@ZAVCl. The quantum efficiencies (QE) of both materials also follow a similar trend (1.32% of CdS@ZAVCl MOF vs 0.42% of thioglycolic acid capped CdS). The inefficiency of ZAVCl-MOF can be ascribed to its colorless, transparent nature, which makes it incapable of absorbing visible light. Diffuse reflectance spectra of ZAVCl-MOF also support this argument, as it shows only one prominent peak in the short-UV region (265 nm; Figure S4e, Supporting Information). To determine the possible paths for the transfer of charge carriers in the case of CdS@ZAVCl, Mott–Schottky (MS) measurements were performed on ZAVCl-MOF using electrochemical impedance techniques (details of the Mott–Schottky experiment can be found in the Supporting Information, section S1-D). A wide band gap of 3.9 eV (Figure S7a,b, Supporting Information) and a positive slope of the MS plot[12i] confirm MOF to be an n-type wide band gap semiconductor. Mott–Schottky analysis gives a flat band potential of MOF (found to be 0.59 V vs. NHE; Figure S7c, Supporting Information). It is well known that the flat band potential of an n-type semiconductor equals its Fermi level.[12j] The conduction band edge of such n-type semiconductors is more negative by about 0.10 V than the flat band potential.[12k] Thus, the conduction band of ZAVCl MOF can be estimated to be −0.491 V vs NHE. Hence, the low-lying conduction band edge of MOF (−0.491 V vs NHE) in comparison to CdS (−0.65 V vs NHE)[12b,c] favors the stabilization of CdS photoelectrons on MOF, which thereby results in an efficient charge separation. However, CdS@ZAVCl MOF is found to be incapable of splitting water, consequent to the well-known problem of sluggish reaction kinetics on the surface of photocatalysts.[12g,h] Pt (0.5 wt % of the CdS@ZAVCl MOF) cocatalyst conventionally acts as an electron sink apart from rendering effective sites for reduction of hydrogen, which thereby decreases the activation energy for the reduction of protons[12g,h] (the mechanism of photocatalytic water splitting has been described in a detailed manner in section S6 in the Supporting Information). The CdS@ZAVCl MOF exhibits stable photocatalytic activity for multiple cycles (Figure 4f).

dx.doi.org/10.1021/ja509019k | J. Am. Chem. Soc. 2014, 136, 14845–14851

There exist few reports in the literature in regard to the photocatalytic water-splitting ability of MOFs (mainly MOF-CdS composite material).[12b,c] However, none of them provide a more easily viable synthetic method than that of CdS@ZAVCl MOF, as all of them require high temperature and a much longer time for synthesis. Moreover, the CdS@ZAVCl MOF exhibits considerably good performance in H_2 production although being loaded with a very small amount of photosensitizing agent (the loading of CdS is ∼1 wt %).[12b,c] It is noteworthy that the CdS@ZAVCl MOF performs more efficiently as a photocatalyst (H_2 evolution 500−510 μmol h^{-1} g^{-1}) in the presence of UV light (i.e., UV + vis; light source without UV filter). In the absence of a UV filter, the incident radiation contains photons of all wavelengths in the visible as well as UV region. The range of photons that could be now absorbed by CdS quantum dots increases considerably (i.e., 370 nm < λ < 440 nm). The increment in the amount of photons absorbed thereby increases the number of photoelectron−hole pairs generated, which in turn escalates the hydrogen evolution (H_2 evolution 500−510 μmol h^{-1} g^{-1}).

In summary, we have prepared a CdS quantum dot based gel material (CdS@ZAVA gel) in a unique one-pot procedure at room temperature. Unlike other methods, this synthesis cum entrapment procedure of CdS does not require any capping agent to stabilize it in the gel matrix. The gel shows tunable luminescence with time, owing to gradual increments in the size of CdS in the gel matrix. However, the luminescence color becomes persistent as we solidify the CdS@ZAVA gel by means of converting it into xerogel. The CdS incubated ZAVA gel can easily be transformed into a CdS loaded MOF by simple addition of chloride salt (e.g.NaCl, KCl, NH_4Cl, etc.).These CdS embedded MOFs can be utilized as photocatalysts in visible light water-splitting reactions. This method not only shows a simple way to make high-quality single crystals but also immobilization of dopants in the matrix of gel, xerogel, and MOF which might lead to the construction of functional composite materials.

■ ASSOCIATED CONTENT

Ⓢ Supporting Information

Text, figures, and tables giving synthetic procedures and PXRD, FT-IR, TGA, and luminescence data. This material is available free of charge via the Internet at http://pubs.acs.org.

■ AUTHOR INFORMATION

Corresponding Author

*E-mail for R.B.: r.banerjee@ncl.res.in.

Notes

The authors declare no competing financial interest.

■ ACKNOWLEDGMENTS

S.S. acknowledges the CSIR for an SRF. G.D. acknowledges CSIR's XIIth Five Year Plan Project for an RA fellowship. J.T. acknowledges the CSIR for CSIR-Nehru postdoctoral fellowship. R.B. acknowledges CSC0122 and CSC0102 for funding. Financial assistance from the DST (SB/S1/IC-32/2013) is acknowledged. We thank Ms. Harshitha Barike Aiyappa, Dr. Sreekumar Kurungot for Mott−Schottky studies, and Mr. Krishna Gavvala and Dr. Partha Hazra for fluorescent lifetime measurements. We also thank Mr. Joyashish Debgupta, Mr. Avik Banerjee, Ms. Meenal Deo, Dr. Satishchandra B. Ogale, and Dr. Chinnakonda S. Gopinath for useful discussions.

■ REFERENCES

(1) (a) Díaz, D. D.; Kühbeck, D.; Koopmans, R. J. *Chem. Soc. Rev.* **2011**, *40*, 427. (b) Fatás, P.; Bachl, J.; Oehm, S.; Jiménez, A. I.; Cativiela, C.; Díaz, D. D. *Chem. Eur. J.* **2013**, *19*, 8861. (c) Weiss, R. G.; Abdallah, D. J. *Adv. Mater.* **2000**, *12*, 1237. (d) Terech, P.; Weiss, R. G. *Chem. Rev.* **1997**, *97*, 3133−3160. (e) Weiss, R. G. *J. Am. Chem. Soc.* **2014**, *136*, 7519. (f) Steed, J. W. *Chem. Soc. Rev.* **2010**, *39*, 3686. (g) Kumar, D. K.; Steed, J. W. *Chem. Soc. Rev.* **2014**, *43*, 2080. (h) Meazza, L.; Foster, J. A.; Fucke, K.; Metrangolo, P.; Resnati, G.; Steed, J. W. *Nat. Chem.* **2013**, *5*, 42.

(2) (a) Zhou, J.; Du, X. W.; Gao, Y.; Shi, J. F.; Xu, B. *J. Am. Chem. Soc.* **2014**, *136*, 2970. (b) Zhang, Y.; Zhang, B.; Kuang, Y.; Gao, Y.; Shi, J.; Zhang, X. X.; Xu, B. *J. Am. Chem. Soc.* **2013**, *135*, 5008. (c) Wang, Q.; Maynar, J. L.; Yoshida, M.; Lee, E.; Lee, M.; Okuro, K.; Kinbara, K.; Aida, T. *Nature* **2010**, *463*, 339. (d) Tamesue, S.; Ohtani, M.; Yamada, K.; Ishida, Y.; Spruell, J. M.; Lynd, N. A.; Hawker, C. J.; Aida, T. *J. Am. Chem. Soc.* **2013**, *135*, 15650. (e) Harada, A.; Kobayashi, R.; Takashima, Y.; Hashidzume, A.; Yamaguchi, H. *Nat. Chem.* **2011**, *3*, 34. (f) Yamaguchi, H.; Kobayashi, Y.; Kobayashi, R.; Takashima, Y.; Hashidzume, A.; Harada, A. *Nat. Commun.* **2012**, *3*, 603. (g) Dastidar, P. *Chem. Soc. Rev.* **2008**, *37*, 2699.

(3) (a) Vermonden, T.; Censi, R.; Hennink, W. E. *Chem. Rev.* **2012**, *112*, 2853. (b) Appel, E.; A. Barrio, J. del.; Loh, X. J.; Scherman, O. A. *Chem. Soc. Rev.* **2012**, *41*, 6195. (c) Banerjee, S.; Das, R. K.; Maitra, U. *J. Mater. Chem.* **2009**, *19*, 6649. (d) Estroff, L. A.; Hamilton, A. D. *Chem. Rev.* **2004**, *104*, 1201.

(4) (a) Palui, G.; Nanda, J.; Ray, S.; Banerjee, A. *Chem. Eur. J.* **2009**, *15*, 6902. (b) Wadhavane, P. D.; Galian, R. E.; Izquierdo, M. A.; Aguilera Sigalat, J.; Galindo, F.; Schmidt, L.; Burguete, M. I.; Perez-Prieto, J.; Luis, S. V. *J. Am. Chem. Soc.* **2012**, *134*, 20554. (c) Chakrabarty, A.; Maitra, U.; Das, A. D. *J. Mater. Chem.* **2012**, *22*, 18268.

(5) Cametti, M.; Džolić, Z. *Chem. Commun.* **2014**, *50*, 8273.

(6) Yuan, J.; Wen, D.; Gaponik, N.; Eychmüller, A. *Angew. Chem., Int. Ed.* **2013**, *52*, 976.

(7) (a) Chae, H. K.; Siberio-Perez, D. Y.; Kim, J.; Go, Y.; Eddaoudi, M.; Matzger, A. J.; O'Keeffe, M.; Yaghi, O. M. *Nature* **2004**, *427*, 523. (b) Furukawa, H.; Cordova, K. E.; O'Keeffe, M.; Yaghi, O. M. *Science* **2013**, *341*, 1230444. (c) Furukawa, H.; Gándara, F.; Zhang, Y.-B.; Jiang, J.; Queen, W. L.; Hudson, M. R.; Yaghi, O. M. *J. Am. Chem. Soc.* **2014**, *136*, 4369. (d) Lee, J. Y.; Farha, O. K.; Roberts, J.; Scheidt, K. A.; Nguyen, S. T.; Hupp, J. T. *Chem. Soc. Rev.* **2009**, *38*, 1450. (e) Guillerm, V.; Weseliński, Ł. J.; Belmabkhout, Y.; Cairns, A. J.; D'Elia, V.; Wojtas, Ł.; Adil, K.; Eddaoudi, M. *Nat. Chem.* **2014**, *6*, 673. (f) Alkordi, M. H.; Brant, J. A.; Wojtas, L.; Kravtsov, V. C.; Cairns, A. J.; Eddaoudi, M. *J. Am. Chem. Soc.* **2009**, *131*, 17753. (g) Li, P.; He, Y.; Guang, J.; Weng, L.; Zhao, J. C.-G.; Xiang, S.; Chen, B. *J. Am. Chem. Soc.* **2014**, *136*, 547. (h) Schoedel, A.; Scherb, C.; Bein, T. *Angew. Chem., Int. Ed.* **2010**, *49*, 7225. (i) Scherb, C.; Schoedel, A.; Bein, T. *Angew. Chem., Int. Ed.* **2008**, *47*, 5777. (j) Senkovska, I.; Kaskel, S. *Chem. Commun.* **2014**, *50*, 7089. (k) Schneemann, A.; Bon, V.; Schwedler, I.; Senkovska, I.; Kaskel, S.; Fischer, R. A. *Chem. Soc. Rev.* **2014**, *43*, 6062. (l) Yang, S.; Sun, J.; Ramirez-Cuesta, A. J.; Callear, S. K.; David, W. I. F.; Anderson, D. P.; Newby, R.; Blake, A. J.; Parker, J. E.; Tang, C. C.; Schröder, M. *Nat. Chem.* **2012**, *4*, 887. (m) Cravillon, J.; Munzer, S.; Lohmeier, S. J.; Feldhoff, A.; Huber, K.; Wiebcke, M. *Chem. Mater.* **2009**, *21*, 1410. (n) Zhuang, J. L.; Ceglarek, D.; Pethuraj, S.; Terfort, A. *Adv. Funct. Mater.* **2011**, *21*, 1442. (o) Friščić, T.; Halasz, I.; Beldon, P. J.; Belenguer, A. M.; Adams, F.; Kimber, S. A. J.; Honkimaki, V.; Dinnebier, R. E. *Nat. Chem.* **2013**, *5*, 66. (p) Dey, C.; Kundu, T.; Biswal, B. P.; Mallick, A.; Banerjee, R. *Acta Cryst. B* **2014**, *70*, 3.

(8) (a) Yan, Y.; Bein, T. *J. Am. Chem. Soc.* **1995**, *117*, 9990. (b) Bein, T.; Brown, K. *J. Am. Chem. Soc.* **1989**, *111*, 7640. (c) Desiraju, G. R.; Curtin, D. Y.; Paul, I. C. *J. Am. Chem. Soc.* **1977**, *99*, 6148.

(9) Yaghi, O. M.; Li, G.; Li, H. *Chem. Mater.* **1997**, *9*, 1074.

(10) Foster, J. A.; Piepenbrock, M.O. M.; Lloyd, G. O.; Clarke, N.; Howard, J. A. K.; Steed, J. W. *Nat. Chem.* **2010**, *2*, 1037.

(11) (a) Lu, G.; Li, S. Z.; Guo, Z.; Farha, O. K.; Hauser, B. G.; Qi, X. Y.; Wang, Y.; Wang, X.; Han, S. Y.; Liu, X. G.; DuChene, J. S.; Zhang, H.; Zhang, Q. C.; Chen, X. D.; Ma, J.; Loo, S. C. J.; Wei, W. D.; Yang, Y. H.; Hupp, J. T.; Huo, F. W. *Nat. Chem.* **2012**, *4*, 310. (b) Jin, S.; Son, H.-J.; Farha, O. K.; Wiederrecht, G. P.; Hupp, J. T. *J. Am. Chem. Soc.* **2013**, *135*, 955. (c) Buso, D.; Jasieniak, J.; Lay, M. D. H.; Schiavuta, P.; Scopece, P.; Laird, J.; Amenitsch, H.; Hill, A. J.; Falcaro, P. *Small* **2012**, *8*, 80.

(12) (a) Li, Q.; Guo, B. D.; Yu, J. G.; Ran, J. R.; Zhang, B. H.; Yan, H. J.; Gong, J. R. *J. Am. Chem. Soc.* **2011**, *133*, 10878. (b) Lin, R.; Shen, L.; Ren, Z.; Wu, W.; Tan, Y.; Fu, H.; Zhang, J.; Wu, L. *Chem. Commun.* **2014**, *50*, 8533. (c) He, J.; Yan, Z.; Wang, J.; Xie, J.; Jiang, L.; Shi, Y.; Yuan, F.; Yu, F.; Sun, Y. *Chem. Commun.* **2013**, *49*, 6761. (d) Kataoka, Y.; Sato, K.; Miyazaki, Y.; Masuda, K.; Tanaka, H.; Naito, S.; Mori, W. *Energy Env. Sci.* **2009**, *2*, 397. (e) Wang, C.; deKrafft, K. E.; Lin, W. *J. Am. Chem. Soc.* **2012**, *134*, 7211. (f) Nasalevich, M. A.; van der Veen, M.; Kapteijn, F.; Gascon, J. *CrystEngComm* **2014**, *16*, 4919. (g) Yang, J.; Wang, D.; Han, H.; Li, C. *Acc. Chem. Res.* **2013**, *46*, 1900. (h) Ran, J.; Zhang, J.; Yu, J.; Jaroniecc, M.; Qiao, S. Z. *Chem. Soc. Rev.* **2014**, DOI: 10.1039/c3cs60425j. (i) Gelderman, K.; Lee, L.; Donne, S. W. *J. Chem. Educ.* **2007**, *84*, 685. (j) An, X.; Yu, X.; Yu, J. C.; Zhang, G. *J. Mater. Chem. A* **2013**, *1*, 5158. (k) He, J.; Wang, J.; Chen, Y.; Zhang, J.; Duan, D.; Wangand, Y.; Yan, Z. *Chem. Commun.* **2014**, *50*, 7063.

(13) (a) Saha, S.; Bachl, J.; Kundu, T.; Díaz, D. D.; Banerjee, R. *Chem. Commun.* **2014**, *50*, 3004. (b) Saha, S.; Bachl, J.; Kundu, T.; Díaz, D. D.; Banerjee, R. *Chem. Commun.* **2014**, *50*, 7032. (c) Sahoo, S. C.; Kundu, T.; Banerjee, R. *J. Am. Chem. Soc.* **2011**, *133*, 17950.

(14) Passerini, S.; Chang, D.; Chu, X.; Le, D. B.; Smyrl, W. *Chem. Mater.* **1995**, *7*, 780 and references therein.

(15) (a) Desiraju, G. R.; Steiner, T. *The Weak Hydrogen Bond in Structural Chemistry and Biology*; Oxford University Press: Oxford, U.K., 1999.

(16) Kamlet, M. J.; Abboud, J. L. M.; Abraham, M. H.; Taft, R. W. *J. Org. Chem.* **1983**, *48*, 2877.

(17) This phenomenon can be attributed to the coordination environment of the probable gelator complex. ZNVA and ZPVA contain four water molecules in their coordination environment (the other two are occupied by the carboxylate of ligand VA), whereas ZAVA accommodates only two water molecules (the other four are occupied by two carboxylates from acetate and VA ligand). Now, according to the HSAB principle, Zn^{2+} is a soft-to-borderline acid and prefers acetate (medium field ligand) over H_2O (stronger than acetate). Hence, ZNPA/ZPVA becomes more vulnerable than ZAVA in the presence of sulfide, which leads to quick precipitation of ZnS.

(18) Lesnyak, V.; Voitekhovich, S. V.; Gaponik, P. N.; Gaponik, N.; Eychmüller, A. *ACS Nano* **2010**, *4*, 4090.

(19) Berti, L.; Burley, G. A. *Nat. Nanotechnol.* **2008**, *3*, 81.

(20) http://hyperphysics.phy-astr.gsu.edu/hbase/vision/cie.html.